

Special
Collection

Olaparib-Based Photoaffinity Probes for PARP-1 Detection in Living Cells

Jim Voorneveld,^[a] Bogdan I. Florea,^{*[a]} Thomas Bakkum,^[a] Rafal J. Mendowicz,^[a] Miriam S. van der Veer,^[a] Berend Gagstein,^[a] Sander I. van Kasteren,^[a] Mario van der Stelt,^[a] Herman S. Overkleeft,^[a] and Dmitri V. Filippov^{*[a]}

The poly-ADP-ribose polymerase (PARP) is a protein from the family of ADP-ribosyltransferases that catalyzes polyadenosine diphosphate ribose (ADPR) formation in order to attract the DNA repair machinery to sites of DNA damage. The inhibition of PARP activity by olaparib can cause cell death, which is of clinical relevance in some tumor types. This demonstrates that quantification of PARP activity in the context of living cells is of great importance. In this work, we present the design, synthesis and biological evaluation of photo-activatable affinity probes inspired by the olaparib molecule that are equipped with a diazirine for covalent attachment upon activation by UV light and a ligation handle for the addition of a reporter group of choice. SDS-PAGE, western blotting and label-free LC-MS/MS quantification analysis show that the probes target the PARP-1 protein and are selectively outcompeted by olaparib; this suggests that they bind in the same enzymatic pocket. Proteomics data are available via ProteomeXchange with identifier PXD018661.

One of the crucial steps in the repair of DNA double-strand breaks is ADP-ribosylation of chromatin,^[1–6] a process driven by several members of the PARP family^[7–9] otherwise known as ARTDs (poly-ADP-ribosyltransferases).^[10] This family of transferases represents clinically relevant target proteins for drugs directed to tumors that are deficient in their DNA repair.^[11,12] The ability to monitor ARTDs *in vivo* is necessary if one wants to study the processes of the drug-target engagement and pharmacokinetics. Small molecule probes that are capable to specifically and covalently bind to their target enzymes in living

cells and in tissues have been developed for various classes of enzymes^[13–17] and used in successful studies involving *in vivo* protein detection and quantification. One way to attain such a probe is to convert a known reversible enzyme inhibitor into a covalent probe suitable for affinity-based protein profiling (AfBPP).^[17–20] AfBPP probes consist of a recognition element that reversibly interacts with the target of interest on which a photoreactive group and ligation handle are installed, without affecting the affinity of the parent structure. Irradiation by UV light activates the photoreactive group, forming a covalent bond between the probe and the target protein in the process called photo-affinity labeling (PAL).^[19–22] The bioorthogonal ligation handle is used to couple a reporter group, such as a fluorophore for in-gel analysis or a biotin for affinity enrichment, with subsequent tandem mass spectrometry in chemical proteomics. In this work we present such a covalent probe for the detection of PARP-1 in live cells using AfBPP (Figure 1). Prior work on the detection of PARP was focused solely on non-covalently binding molecules with the aim of either off-target finding^[23,24] or *in vivo* imaging.^[25,26] We set out to design, synthesize and biologically validate a PARP-1-selective photoaffinity probe for use in the standard proteomics protocols. Such well-established workflows make use of UV-induced PAL through a diazirine tag and copper-catalyzed alkyne-azide cycloaddition that enable the pull-down of the protein for subsequent analysis by standard mass-spectrometry methods.

The clinical PARP inhibitor olaparib was chosen as the starting point for the design of the recognition element of photoaffinity probes **3** and **6**, because it inhibits PARP-1 and PARP-2 with a nanomolar potency and shows exceptional selectivity over other cellular targets.^[24,27,28] The synthesis of **3** and **6** is depicted in Scheme 1. For PAL, a plethora of photo reactive groups is reported.^[29] In order to limit the interference of the tag with the activity and selectivity of the probes, we chose the compact diazirine-alkyne linkers **2** and **5** developed by Li et al.^[30] The nitrogen atom of the piperazine moiety distal from the phtalazinone substructure of olaparib is known to tolerate a wide range of modifications.^[28,31] With this in mind, we attached the photoaffinity tag to this nitrogen to minimize its influence on binding efficiency to PARP-1, giving the design of probe **3**. A second, simplified probe **6**, in which we removed the piperazine bridge and attached the diazirine-alkyne tag directly to benzylphtalazinone core of the olaparib structure was also synthesized. The probes were prepared by HCTU-mediated condensation of either commercially available **1** or known compound **4**^[25,28] with the linkers **2** and **5**, respectively.

[a] J. Voorneveld, Dr. B. I. Florea, T. Bakkum, R. J. Mendowicz, M. S. van der Veer, B. Gagstein, Dr. S. I. van Kasteren, Prof. Dr. M. van der Stelt, Prof. Dr. H. S. Overkleeft, Dr. D. V. Filippov
Bio-organic Synthesis Group
Leiden Institute of Chemistry, Leiden University
Einsteinweg 55, 2333 CC Leiden (The Netherlands)
E-mail: b.florea@chem.leidenuniv.nl
filippov@chem.leidenuniv.nl

Supporting information for this article is available on the WWW under <https://doi.org/10.1002/cbic.202000042>

This article is part of a Special Collection on Chemical Proteomics and Metabolomics. To view the complete collection, visit our homepage

© 2020 The Authors. Published by Wiley-VCH Verlag GmbH & Co. KGaA. This is an open access article under the terms of the Creative Commons Attribution Non-Commercial NoDerivs License, which permits use and distribution in any medium, provided the original work is properly cited, the use is non-commercial and no modifications or adaptations are made.

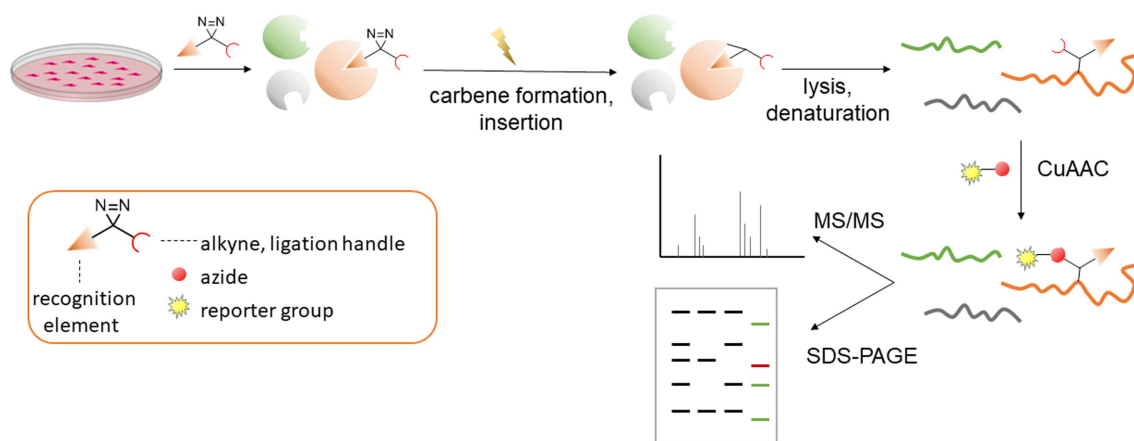
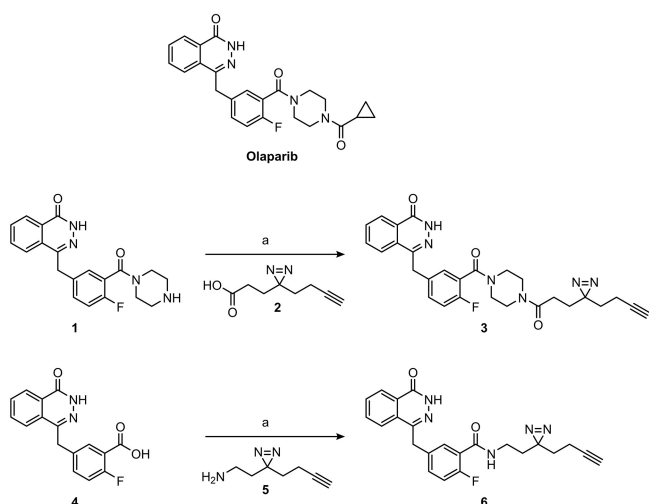


Figure 1. Live Raji cells were treated with probe **3** or **6**. Irradiation at 350 nm activates the diazirine group, forming a highly reactive carbene that can rapidly insert into nearby N–H, O–H or C–H bonds. Protein extraction was done by cell lysis under denaturing conditions. Reporter or affinity handles were introduced by CuAAC click chemistry. Proteins were analyzed by SDS-PAGE and/or western blot or by affinity purification, digested to peptides and LFQ proteomics analysis.



Scheme 1. Structure of olaparib and the synthesis of the derived probes **3** and **6**. a) HCTU, DIPEA, DMF, 33% for **3**, 75% for **6**.

With the AfBPs **3** and **6** in hand, their ability to bind PARP covalently through PAL in live cells was tested on the human B-cell-derived Raji cell line. Raji cells were chosen as the model because they are easy to grow in suspension and have an advantageous nucleus-to-cytoplasm ratio that maximizes the PARP abundance. The cells were incubated with probes **3** or **6** (10 μM) and irradiated with UV light for 30 minutes to ensure complete activation of the diazirine and covalent labeling of PARP. During irradiation, the cells were cooled to 4 $^{\circ}\text{C}$ to counteract the heat generated from the irradiation. The cells were then harvested and lysed. The lysate was treated with the azide-containing fluorophore AlexaFluor 647 under click conditions and further processed for in-gel fluorescence analysis. The gel revealed a fluorescent band at the expected height of around 116 kDa (Figure 2, lanes 3) which was probe-dependent as cells treated with only the DMSO vehicle (lanes 2) revealed

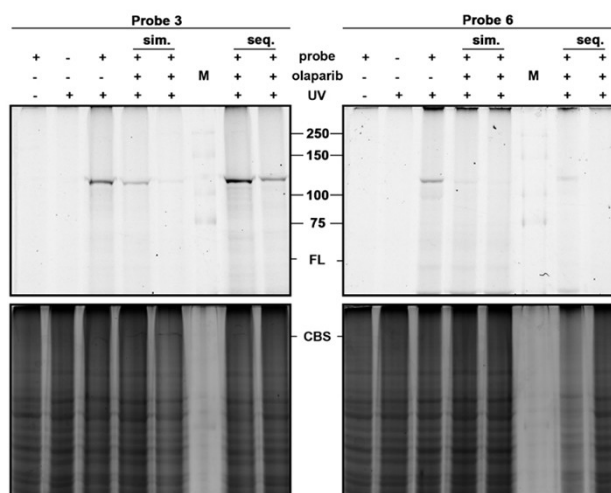


Figure 2. SDS-PAGE analysis and fluorescent imaging of Raji cells exposed to probes **3** and **6** (10 μM) without UV control. sim: simultaneous incubation at a 1:1 (10 μM olaparib, 10 μM probe) or 5:1 (50 μM olaparib, 10 μM probe) ratio. seq: sequential incubation with olaparib, wash and probe at 1:1 ratio or 2:1 olaparib/probe ratio. FL: fluorescence channel. CBS: Coomassie Blue staining for loading control of the gel in the upper panel. M: protein ladder

no labeling. The same cell lysates were also coupled to diazo biotin-azide (DBA, Figure S4 in the Supporting Information) and an anti-biotin western-blot (WB) revealed the same band at 116 kDa (Figure S1) verifying that the detected bands are probe-specific. To further show probe-specific labeling, the UV irradiation step was omitted yielding no signal, showing that the observed labeling is UV-dependent rather than circumstantial activation. As an additional control, the gel used for in-gel fluorescence readout was analyzed by western blot with an anti-PARP-1 antibody showing bands at the same height confirming it to be PARP-1 (Figure S1). To further verify our target, we performed a click reaction with *N*-(3-azidopropyl) biotinamide (Figure S5) on the lysates and enriched the probe-

bound proteins on streptavidin beads. SDS-PAGE followed by WB analysis with the anti-PARP-1 antibody proved the probe-bound protein to be PARP-1 (Figure S2).

Having verified that probes **3** and **6** were able to label PARP in a UV-dependent covalent manner, we reasoned they should also be outcompeted by olaparib, as they should bind to the same protein active site. The probes and olaparib were incubated simultaneously in a 1:1 ratio after which a decrease of band intensity was observed (lanes 4). After increasing the amount of olaparib to a 5:1 drug/probe ratio, labeling by the probe was fully diminished (lanes 5). Interestingly, in a sequential competition experiment where first olaparib was administered, removed and then incubated with the probes in a 1:1 ratio, no apparent competition was observed (lanes 7) and when a 2:1 drug/probe ratio was applied, the bands appeared to decrease slightly (lanes 8) but proved not as effective as simultaneous competition. This effect might be due to rapid dissociation of olaparib from the PARP binding pocket during the washing step.

Next, we wanted to show the probes ability to bind PARP in conditions frequently encountered in the field of ADP-ribosylation research. H₂O₂ is often used to induce double strand breaks, facilitating PARP activation. Therefore, Raji cells were treated with the probes as before with addition of H₂O₂ during incubation. The addition of this oxidizing agent neither changed the ability of the probes to label PARP nor the

efficiency of the labeling (Figure S3). The latter result suggests that olaparib is able to bind to PARP in the absence of extensive DNA-damage and appears consistent with previously reported findings.^[23]

To identify and quantify the bands seen by SDS-PAGE and western blot analysis we used a LC-MS/MS-based label-free quantification (LFQ) method.^[16] The results show that PARP-1 is significantly UV-enriched by probe **3**, thus indicating that the observed band at 116 kDa can be attributed to PARP-1 (Figure 3A and B). Competition analysis of significantly UV-enriched proteins shows that PARP-1 is outcompeted by olaparib (Figure 3D); this strongly indicates that the probe binds in the same protein pocket as olaparib. Several other proteins were selectively enriched by the probe upon UV irradiation indicating that the probe targets these proteins possibly by their nucleic acid binding or perhaps by the presence of the diazirine group (Figure 3C).^[33] PARP-1 was not significantly UV enriched by probe **6** (Figure S6), which agrees with the in-gel fluorescence data for this probe that showed fainter bands for PARP-1 compared with the background. Apparently, removal of the piperazine ring diminishes the binding affinity of probe **6** to PARP-1.

In conclusion, we present for the design and synthesis of two synthetically accessible olaparib-based photoaffinity probes (**3** and **6**) for PARP-1 detection in living cells. We show evidence

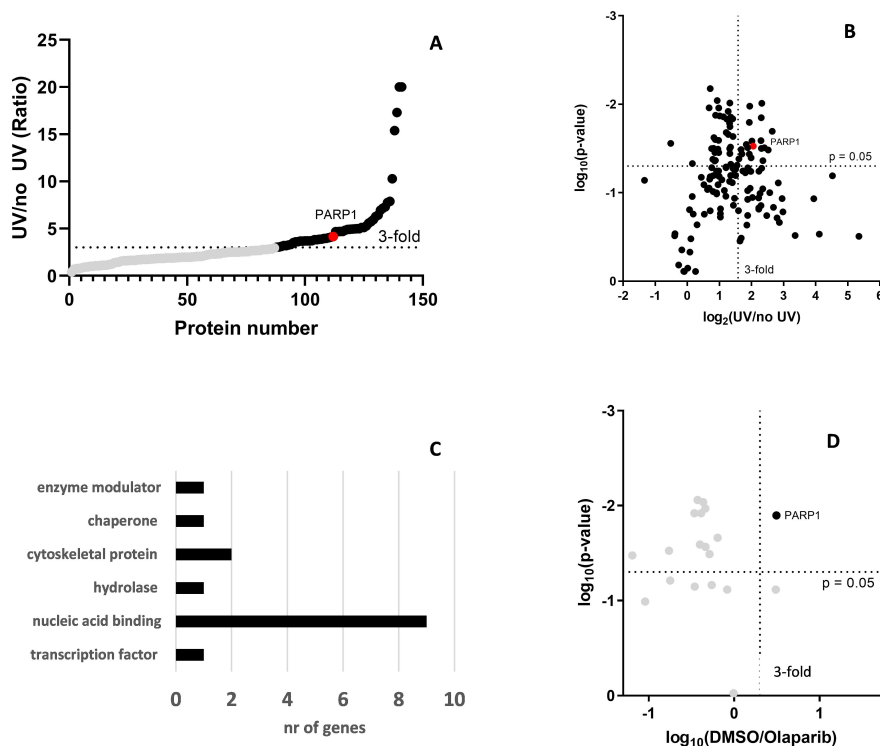


Figure 3. LFQ proteomics analysis of probe **3** in living Raji cells of proteins with at least two unique peptides. A) Waterfall plot of UV enrichment by probe **3** of proteins identified in the proteomics analysis, proteins showing a more than threefold UV enrichment are in black. B) Volcano plot of UV enrichment of proteins by probe **3**, proteins showing a more than threefold UV enrichment and with $p < 0.05$ using a Student's *t*-test are in black. PARP-1 is marked in red. C) Significantly UV-enriched proteins sorted with the gene function analysis module of the PANTHER classification system (v.14.0) software.^[32] D) Competition analysis of significantly UV-enriched probe targets, proteins outcompeted more than threefold by olaparib pre-addition with $p < 0.05$ using a Student's *t*-test are in black.

of efficacy and provide a detailed protocol for application of these probes. Both **3** and **6** proved to be stable under oxidative conditions often employed for PARP activation while probe **3** was successfully used to label PARP-1 selectively in a live-cell model and to analyze its presence by in-gel fluorescence and LFQ LC-MS/MS methods.

The mass spectrometry proteomics data have been deposited with the ProteomeXchange Consortium via the PRIDE^[35] partner repository with the dataset identifier PXD018661.

Note added in proof

While this paper was under review, a similar approach for PARP-targeting was published by Tate and co-workers.^[34]

Acknowledgements



We are grateful to Ivan Ahel and Thomas Agnew from The Sir William Dunn School of Pathology at the University of Oxford for scientific advice on the *in vitro* experiments. We acknowledge ChemAxon for kindly providing the Instant JChem software to manage our compound library.

Conflict of Interest

The authors declare no conflict of interest.

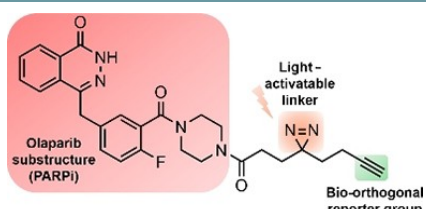
Keywords: bioorthogonal chemistry · chemical proteomics · olaparib · PARP-1 · photoaffinity probes

- [1] S. Messner, M. O. Hottiger, *Trends Cell Biol.* **2011**, *21*, 534–542.
- [2] K. Ueda, A. Omachi, M. Kawaiichi, O. Hayaishi, *Proc. Natl. Acad. Sci. USA* **1975**, *72*, 205–209.
- [3] T. Boulikas, *Proc. Natl. Acad. Sci. USA* **1989**, *86*, 3499–3503.
- [4] A. Huletsky, C. Niedergang, A. Fréchet, R. Aubin, A. Gaudreau, G. G. Poirier, *Eur. J. Biochem.* **1985**, *146*, 277–285.
- [5] N. A. Berger, G. W. Sikorski, *Biochemistry* **1981**, *20*, 3610–3614.
- [6] E. G. Miller, *BBA Sect. Nucleic Acids Protein Synth.* **1975**, *395*, 191–200.
- [7] S. Messner, M. Altmeyer, H. Zhao, A. Pozivil, B. Roschitzki, P. Gehrig, D. Rutishauser, D. Huang, A. Cafilisch, M. O. Hottiger, *Nucleic Acids Res.* **2010**, *38*, 6350–6362.
- [8] S. L. Rulten, A. E. O. Fisher, I. Robert, M. C. Zuma, M. Rouleau, L. Ju, G. Poirier, B. Reina-San-Martin, K. W. Caldecott, *Mol. Cell* **2011**, *41*, 33–45.
- [9] B. Lüscher, M. Bütepage, L. Ecker, S. Krieg, P. Verheugd, B. H. Shilton, *Chem. Rev.* **2018**, *118*, 1092–1136.
- [10] M. O. Hottiger, P. O. Hassa, B. Lüscher, H. Schüler, F. Koch-Nolte, *Trends Biochem. Sci.* **2010**, *35*, 208–219.
- [11] C. J. Lord, A. Ashworth, *Science* **2017**, *355*, 1152–1158.
- [12] N. Curtin, *Biochem. Soc. Trans.* **2014**, *42*, 82–88.
- [13] N. Liu, S. Hoogendoorn, B. van de Kar, A. Kaptein, T. Barf, C. Driessen, D. V. Filippov, G. A. van der Marel, M. van der Stelt, H. S. Overkleeft, *Org. Biomol. Chem.* **2015**, *13*, 5147–5157.
- [14] M. P. Baggelaar, H. den Dulk, B. I. Florea, D. Fazio, N. Bernabò, M. Raspa, A. P. A. Janssen, F. Scavizzi, B. Barboni, H. S. Overkleeft, et al., *ACS Chem. Biol.* **2019**, *14*, 2295–2304.
- [15] A. C. M. van Esbroeck, A. P. A. Janssen, A. B. Cognetta, D. Ogasawara, G. Shpak, M. van der Kroeg, V. Kantae, M. P. Baggelaar, F. M. S. de Vrij, H. Deng, et al., *Science* **2017**, *356*, 1084–1087.
- [16] E. J. van Rooden, B. I. Florea, H. Deng, M. P. Baggelaar, A. C. M. van Esbroeck, J. Zhou, H. S. Overkleeft, M. van der Stelt, *Nat. Protoc.* **2018**, *13*, 752–767.
- [17] a) H. Shi, C. Zhang, G. Y. J. Chen, S. Q. Yao, *J. Am. Chem. Soc.* **2012**, *134*, 3001–3014; b) Y. Su, J. Ge, B. Zhu, Y.-G. Zheng, Q. Zhu, S. Q. Yao, *Curr. Opin. Chem. Biol.* **2013**, *17*, 768–775; c) S. Pan, H. Zhang, C. Wang, S. C. L. Yao, S. Q. Yao, *Nat. Prod. Rep.* **2016**, *33*, 612–620.
- [18] M. P. Baggelaar, P. J. P. Chameau, V. Kantae, J. Hummel, K. L. Hsu, F. Janssen, T. van der Wel, M. Soethoudt, H. Deng, H. den Dulk, et al., *J. Am. Chem. Soc.* **2015**, *137*, 8851–8857.
- [19] X. Yang, T. J. M. Michiels, C. de Jong, M. Soethoudt, N. Dekker, E. Gordon, M. van der Stelt, L. H. Heitman, D. van der Es, A. P. IJzerman, *J. Med. Chem.* **2018**, *61*, 7892–7901.
- [20] M. Soethoudt, S. C. Stolze, M. V. Westphal, L. van Stralen, A. Martella, E. J. van Rooden, W. Guba, Z. V. Varga, H. Deng, S. I. van Kasteren, et al., *J. Am. Chem. Soc.* **2018**, *140*, 6067–6075.
- [21] Z. Wang, Z. Guo, T. Song, X. Zhang, N. He, P. Liu, P. Wang, Z. Zhang, *ChemBioChem* **2018**, *19*, 2312–2320.
- [22] M. Jouanneau, B. McClary, J. C. P. Reyes, R. Chen, Y. Chen, W. Plunkett, X. Cheng, A. Z. Milinichik, E. F. Albone, J. O. Liu, et al., *Bioorg. Med. Chem. Lett.* **2016**, *26*, 2092–2097.
- [23] K. S. Yang, G. Budin, C. Tassa, O. Kister, R. Weissleder, *Angew. Chem. Int. Ed.* **2013**, *52*, 10593–10597; *Angew. Chem.* **2013**, *125*, 10787–10791.
- [24] C. E. Knezevic, G. Wright, L. L. Rensing Rix, W. Kim, B. M. Kuenzi, Y. Luo, J. M. Watters, J. M. Koomen, E. B. Haura, A. N. Monteiro, et al., *Cell Chem. Biol.* **2016**, *23*, 1490–1503.
- [25] F. Zmuda, G. Malviya, A. Blair, M. Boyd, A. J. Chalmers, A. Sutherland, S. L. Pimlott, *J. Med. Chem.* **2015**, *58*, 8683–8693.
- [26] T. Reiner, S. Earley, A. Turetsky, R. Weissleder, *ChemBioChem* **2010**, *11*, 2374–2377.
- [27] E. D. Deeks, *Drugs* **2015**, *75*, 231–240.
- [28] K. A. Menear, C. Adcock, R. Boulter, X. L. Cockcroft, L. Copsey, A. Cranston, K. J. Dillon, J. Drzewiecki, S. Garman, S. Gomez, et al., *J. Med. Chem.* **2008**, *51*, 6581–6591.
- [29] P. Geurink, L. Prely, G. A. van der Marel, R. Bischoff, H. S. Overkleeft, *Photoaffinity Labeling in Activity-Based Protein Profiling*, In: Sieber S. (eds) *Activity-Based Protein Profiling*. Topics in Current Chemistry, vol 324. Springer, Berlin, Heidelberg **2011**.
- [30] Z. Li, P. Hao, L. Li, C. Y. J. Tan, X. Cheng, G. Y. J. Chen, S. K. Sze, H. M. Shen, S. Q. Yao, *Angew. Chem. Int. Ed.* **2013**, *52*, 8551–8556; *Angew. Chem.* **2013**, *125*, 8713–8718.
- [31] E. Wahlberg, T. Karlberg, E. Kouznetsova, N. Markova, A. Macchiarulo, A. G. Thorsell, E. Pol, Å. Frostell, T. Ekblad, D. Öncü, et al., *Nat. Biotechnol.* **2012**, *30*, 283–288.
- [32] H. Mi, A. Muruganujan, X. Huang, D. Ebert, C. Mills, X. Guo, P. D. Thomas, *Nat. Protoc.* **2019**, *14*, 703–721.
- [33] P. Kleiner, W. Heydenreuter, M. Stahl, V. S. Korotkov, S. A. Sieber, *Angew. Chem.* **2017**, *24*, 1396–1401.
- [34] R. T. Howard, P. Hemsley, P. Petteruti, C. N. Saunders, J. A. Molina Bermejo, J. S. Scott, J. W. Johannes, E. W. Tate, *ACS Chem. Biol.* **2020**, *15*, 325–333.
- [35] Y. Perez-Riverol, A. Csordas, J. Bai, M. Bernal-Llinares, S. Hewapathirana, D. J. Kundu, A. Inuganti, J. Griss, G. Mayer, M. Eisenacher, E. Pérez, J. Uszkoreit, J. Pfeuffer, T. Sachsenberg, S. Yilmaz, S. Tiwary, J. Cox, E. Audain, M. Walzer, A. F. Jarnuczak, T. Ternent, A. Brazma, J. A. Vizcaino, *Nucleic Acids Res.* **2019**, *47*, D442–D450.

Manuscript received: January 24, 2020
 Revised manuscript received: April 11, 2020
 Accepted manuscript online: April 13, 2020
 Version of record online:  

COMMUNICATIONS

Impair the repair: Olaparib is a PARP inhibitor (PARPi) of clinical relevance because it causes cell death in certain tumor types. By using a substructure of olaparib and adding a photo-activatable linker, a proteomics assay is presented for visualizing PARP1 with in-gel fluorescence and MS/MS analysis.



J. Voorneveld, Dr. B. I. Florea, T. Bakkum, R. J. Mendowicz, M. S. van der Veer, B. Gagestein, Dr. S. I. van Kasteren, Prof. Dr. M. van der Stelt, Prof. Dr. H. S. Overkleeft, Dr. D. V. Filippov**

1 – 5

Olaparib-Based Photoaffinity Probes for PARP-1 Detection in Living Cells

